

Inhomogeneous solutions to thermal Hartree-Fock equations in first-order phase transitions

Hikaru Kitamura

Department of Physics, Kyoto University, Sakyo-ku, Kyoto 606-8502, Japan

ABSTRACT

It is shown that the damping algorithm for the density matrix in self-consistent-field iterations, originally proposed for quantum chemistry of molecules in the ground state, can yield convergent solutions to thermal Hartree-Fock equations representing inhomogeneous domain structures in first-order phase transitions. A lattice gas of spinless Fermions with nearest-neighbor attractive interaction is analyzed as an illustration. In the metastable or unstable region of the phase diagram, numerical solutions converge to phase-separated states consisting of gas and liquid domains, characterized by a double-peak structure in the single-particle energy spectrum. Broadening of the energy spectrum due to quantum-mechanical tunneling effect is also demonstrated. The present method would facilitate direct numerical access to phase-transition regions of various quantum/classical systems without causing breakdown.

KEYWORDS

Thermal Hartree-Fock theory; density matrix; first-order phase transition

1. Introduction

The Hartree-Fock (HF) theory at finite temperatures can be formulated on the basis of a variational principle to the grand potential as a functional of the density matrix [1-3]. The HF solution corresponds to a stationary point at which the first derivative of the grand potential vanishes; the second derivative gives a stability criterion that determines whether the solution is stable (i.e., local minimum of free energy) or unstable [2]. Mermin [2] applied this criterion to a classical lattice gas of Fermions with attractive interatomic interactions to show that the instability occurs in the region inside the spinodal lines, which is consistent with the general statistical theory of first-order transitions [2]. His analysis was, however, based on the *homogeneous* HF solutions [2]. Later on, Bondarev [4] formulated a general HF theory of quantum lattice gas with the density matrix; instead of performing numerical calculations, he presented simplified analytical equations of state assuming homogeneous phases to discuss the gas-liquid coexistence. More recently, Mermin's stability analysis has been applied to nuclear matter as well [5].

In the first-order phase transition with a conserved order parameter, phase separation proceeds through nucleation or spinodal decomposition, depending on whether the system is in metastable or unstable region in the phase diagram [6]. In either case, the system eventually reaches an inhomogeneous structure consisting of two types of domains having different densities or concentrations [6,7]. While those inhomogeneous structures have been analysed with coarse-grained statistical models [6] or density-functional theories [8], numerical HF studies of inhomogeneous domain structures have rarely been reported.

Turning our attention to quantum chemistry of molecules, the usual prescription of the HF calculation is to introduce a basis-set expansion of single-particle wavefunctions, and to solve the resultant Roothaan equation iteratively to get a self-consistent solution to the density matrix [9]. It has been pointed out that, during the course of iterations, one may encounter an oscillation of the density matrix between the two states and never get a convergent solution, even for a single atom or a molecule in the ground state [10,11]. To improve convergence of atomic wavefunctions, Hartree [11] originally suggested a simple damping algorithm. Thereafter, various improved algorithms such as the level-shifting method [12], direct inversion

in the iterative subspace [13], optimal damping algorithm [10,14], and their further modifications [14,15] have been proposed for molecules at zero temperature. These works motivate us to study highly unstable statistical systems at finite temperatures with the aid of quantum-chemical formalisms and algorithms.

In this paper, we shall demonstrate numerically that a simplified version of the optimal damping algorithm [10,11,14] enables one to obtain convergent solutions to the thermal HF equations for a lattice gas with nearest-neighbour attractive interactions over the entire density-temperature range. Especially, when the system is in the unstable or metastable region of the first-order phase transition, we obtain inhomogeneous solutions representing phase separation into two phases.

2. Quantum lattice gas

2.1. Thermal Hartree-Fock equations

We consider a quantum lattice gas of N_{atom} identical atoms. The atomic wavefunction $\psi_b(\mathbf{r})$ for single-particle state b is expanded as $\psi_b(\mathbf{r}) = \sum_{i=1}^{N_{\text{site}}} C_{ib} \phi(\mathbf{r} - \mathbf{s}_i)$, where the orbital $\phi(\mathbf{r} - \mathbf{s}_i)$ is assumed to be spherically symmetric and strongly localised at lattice site \mathbf{s}_i ($i = 1, \dots, N_{\text{site}}$). Let us consider the kinetic energy integral $t_{ij} = \int d\mathbf{r} \phi^*(\mathbf{r} - \mathbf{s}_i) \frac{-\hbar^2}{2M} \nabla^2 \phi(\mathbf{r} - \mathbf{s}_j)$, with M denoting the atomic mass. For strongly localised orbitals such that the overlap of neighbouring wavefunctions is small, we may set

$$t_{ii} = \alpha, \quad t_{ij} = \beta \delta_{ij}^{\text{nn}} \quad \text{for } i \neq j, \quad |\alpha| \gg |\beta| \quad (1)$$

where δ_{ij}^{nn} is defined as $\delta_{ij}^{\text{nn}} \equiv 1$ if sites i and j are nearest neighbours to each other, and $\delta_{ij}^{\text{nn}} \equiv 0$ otherwise. We likewise introduce a nearest-neighbour interaction parameter

$$v = \sum_{j=1}^{N_{\text{site}}} \delta_{ij}^{\text{nn}} \int d\mathbf{r} \int d\mathbf{r}' |\phi(\mathbf{r} - \mathbf{s}_i)|^2 v(\mathbf{r} - \mathbf{r}') |\phi(\mathbf{r}' - \mathbf{s}_j)|^2, \quad (2)$$

where $v(\mathbf{r} - \mathbf{r}')$ represents the binary potential between atoms at position \mathbf{r} and \mathbf{r}' .

The atoms are formally treated as spinless Fermions; the Pauli principle then

automatically excludes a possibility that a single site is simultaneously occupied by two or more atoms, similar to the hard-core repulsion assumed in most lattice-gas models [7]. On the basis of the spin-unrestricted version [9] of thermal HF theory [1-3] in conjunction with the neglect of diatomic differential overlap (NDDO) approximation $\phi(\mathbf{r}-\mathbf{s}_i)\phi(\mathbf{r}-\mathbf{s}_j) \approx 0$ for $i \neq j$ [16], the Fock matrix can be written as

$$F_{ii} = \alpha + \frac{v}{z} \sum_{i'(\neq i)}^{N_{\text{site}}} \rho_{i'i'} \delta_{i'i}^{\text{nn}}, \quad (3a)$$

$$F_{ij} = \left[\beta - \frac{v}{z} \rho_{ij} \right] \delta_{ij}^{\text{nn}} \quad \text{for } i \neq j, \quad (3b)$$

where z is the number of nearest-neighbor sites. The exclusion of the contribution $i' = i$ on the right-hand side of Eq. (3a) manifests proper cancellation of self-interaction in the HF theory. We also note that Eq. (3b) originates from the exchange interaction term. The density matrix (or bond-order matrix) at temperature T is given by

$$\rho_{ij} = \sum_b C_{ib} f(\varepsilon_b) C_{jb}^*, \quad (4)$$

with the Fermi distribution,

$$f(\varepsilon) = \frac{1}{e^{(\varepsilon-\mu)/k_{\text{B}}T} + 1}. \quad (5)$$

The chemical potential μ is determined indirectly from the normalisation condition,

$$\sum_b f(\varepsilon_b) = N_{\text{atom}}. \quad \text{Here, accurate determination of } \mu \text{ requires a careful prescription, and we}$$

find it convenient to rewrite this equation as

$$\sum_{b=1}^{N_{\text{atom}}} h(\varepsilon_b) + \sum_{b \geq N_{\text{atom}}+1} f(\varepsilon_b) = 0, \quad (6)$$

where we have introduced a hole function $h(\varepsilon) \equiv f(\varepsilon) - 1$. The summands in the first and second terms on the left-hand side of Eq. (6) are both close to zero and hence no numerical errors can occur. The single-particle energy ε_b and the corresponding expansion coefficients $\{C_{ib}\}$ are obtained through solution to the Roothaan equation [9]

$$\sum_{j=1}^{N_{\text{site}}} F_{ij} C_{jb} = \varepsilon_b C_{ib}. \quad (7)$$

Self-consistent solutions to Eqs. (3)-(7) yield the grand potential [1-3]

$$\Omega = E - TS - \mu N_{\text{atom}}, \quad (8)$$

where

$$E = \frac{1}{2} \sum_{i,j=1}^{N_{\text{site}}} \rho_{ji} (t_{ij} + F_{ij}) \quad (9)$$

is the internal energy, and $S = -k_B \sum_b (1 - f(\varepsilon_b)) \ln(1 - f(\varepsilon_b)) + f(\varepsilon_b) \ln f(\varepsilon_b)$ is the entropy.

We remark in Eq. (3b) that β accounts for quantum tunnelling between neighbouring sites. In the limit $\beta/\alpha \rightarrow 0$, the ordinary classical lattice gas [2,7] is reproduced.

2.2. Damping algorithm

Our task is to solve the matrix form of Eq. (7), $\mathbf{F}(\boldsymbol{\rho})\mathbf{C} = \mathbf{C}\boldsymbol{\varepsilon}$, self-consistently through iterations.

To achieve this in a stable manner, we adopt a damping algorithm. After suitably choosing the initial density matrix $\tilde{\boldsymbol{\rho}}^{\text{in}}$, we repeat the following procedures:

(i) Solve the equation $\mathbf{F}(\tilde{\boldsymbol{\rho}}^{\text{in}})\mathbf{C} = \mathbf{C}\boldsymbol{\varepsilon}$ by diagonalising the matrix \mathbf{F} .

(ii) Calculate $f(\varepsilon_b)$ from the eigenvalue ε in accordance with (5) and (6), which is combined with the eigenvector \mathbf{C} to produce the density matrix (4); the result is denoted as $\boldsymbol{\rho}^{\text{out}}$.

(iii) Compute $\tilde{\boldsymbol{\rho}} \equiv (1 - \lambda)\tilde{\boldsymbol{\rho}}^{\text{in}} + \lambda\boldsymbol{\rho}^{\text{out}}$ and $\mathbf{F}(\tilde{\boldsymbol{\rho}}) \equiv (1 - \lambda)\mathbf{F}(\tilde{\boldsymbol{\rho}}^{\text{in}}) + \lambda\mathbf{F}(\boldsymbol{\rho}^{\text{out}})$, where λ is a damping parameter between 0 and 1.

(iv) The resultant $\tilde{\boldsymbol{\rho}}$ and $\mathbf{F}(\tilde{\boldsymbol{\rho}})$ are redefined as $\tilde{\boldsymbol{\rho}}^{\text{in}}$ and $\mathbf{F}(\tilde{\boldsymbol{\rho}}^{\text{in}})$, respectively, and go to (i).

Here, the tilde symbol stands for a ‘pseudo-density matrix’ [10,14] which is distinguished from the true density matrix defined by (4). The equality $\tilde{\boldsymbol{\rho}}^{\text{in}} = \boldsymbol{\rho}^{\text{out}} = \boldsymbol{\rho}$ is finally attained upon convergence.

We note in (iii) that the case $\lambda = 1$ is equivalent to the neglect of damping, whereas $\lambda \rightarrow 0$ corresponds to strong damping. In the optimal damping algorithm [10,14] proposed originally for molecules at $T = 0$, λ has been optimised in each iteration so as to minimise the total energy E as a function of the idempotent matrix $\tilde{\boldsymbol{\rho}}$. Mathematical foundation of this method and the acceleration of convergence for real molecules have been reported [10,14]. At

finite temperatures, formal justification of the damping procedure is lacking; it is not obvious whether $\mathbf{F}(\tilde{\rho})$ can be minimised with respect to the pseudo-density matrix of the form given by Eq. (4). In the present work, rigorous proof of the damping method at finite temperatures is not pursued. Since we treat even more unstable systems in the presence of thermal effects and phase transitions, our primary concern is to obtain convergent solutions irrespective of the computational speed. We thus adopt a simpler prescription analogous to Hartree's damping method [11] such that λ is kept constant throughout the simulation run.

2.3. Numerical calculations

We carry out numerical calculations for a lattice gas in one dimension ($z = 2$) with $N_{\text{site}} = 40$, imposing the periodic boundary condition. Although a one-dimensional system should not display phase transitions [7], the present HF theory predicts a gas-liquid transition if the interaction is attractive ($v < 0$), which is a well-known drawback of the mean-field treatment. Nevertheless, we shall demonstrate a one-dimensional case for illustrative purposes; our basic equations (3)-(7) remain the same for higher dimensions as well. For a lattice gas of ordinary atoms, the de Broglie wavelength $\Lambda \equiv \hbar / \sqrt{M|v|}$ may be much shorter than the nearest-neighbour distance d . Assuming that $\alpha \sim \hbar^2 / Md^2$, we may estimate roughly as $|v|/\alpha \sim (d/\Lambda)^2 > 1$. Accordingly, the interaction parameter is chosen as $v/\alpha = -5$ throughout this paper.

We shall mainly consider a nearly classical case, $\beta/\alpha = -0.01$. We note that the sign of β/α can affect the sign of the off-diagonal density matrices but does not affect the resultant thermodynamic quantities. Validity of the numerical calculations can be checked through comparison with the known analytical results for the homogeneous phase in the classical mean-field theory [2,7]:

$$\frac{\Omega}{N_{\text{site}}} = k_{\text{B}}T \ln(1 - \bar{f}) + \frac{|v|}{2} \bar{f}^2, \quad (10)$$

$$\mu = k_{\text{B}}T \ln \frac{\bar{f}}{1 - \bar{f}} + \alpha - |v| \bar{f}, \quad (11)$$

where $\bar{f} \equiv N_{\text{atom}} / N_{\text{site}}$ is the average atomic density. Equations (10) and (11) are special solutions to Eqs. (3)-(9) for the case $\beta = 0$, $F_{ii} = \alpha - |v|\bar{f} \equiv \varepsilon$ (independent of i), $\rho_{ij} = F_{ij} = 0$ ($i \neq j$), and $\varepsilon_b = \varepsilon$. In Eq. (11), α is merely a constant additive to μ so that the phase diagram is controlled only by $k_B T / |v|$ and \bar{f} . According to (10) and (11), the gas-liquid critical point is located at $T = T_c = |v| / 4k_B$ and $\bar{f} = f_c = 1/2$ [2,4,7]. We shall mainly study the case $k_B T / |v| = 0.2$, which lies in the phase separation region below T_c . At this temperature, the densities of the coexisting gas and liquid phases are predicted to be $f_{\text{gas}} = 0.145$ and $f_{\text{liq}} = 0.855$, respectively; the spinodal line $\partial\Omega / \partial\bar{f} = 0$ is located at $\bar{f} = 0.276 \equiv f_<$ and $\bar{f} = 0.724 \equiv f_>$ so that the homogeneous phase is unstable for $0.276 < \bar{f} < 0.724$.

Figure 1 illustrates the effects of damping on the evolutions of the density matrix for $\bar{f} = 0.5$. Here, we start to solve Eq. (7) with a nearly homogeneous initial condition $\tilde{\rho}_{ij}^{\text{in}} \approx \bar{f}\delta_{ij}$. When the damping is neglected ($\lambda = 1$), the density matrix immediately begins to oscillate rapidly and never converges, whereas the simulation with $\lambda = 0.5$ leads to a convergent result with $\tilde{\rho}_{ij}^{\text{in}} = \rho_{ij}^{\text{out}} = \rho_{ij}$ after about 50 steps. Stability of the damping method has been confirmed for the other densities and temperatures as well. We adopt $\lambda = 0.5$ throughout this paper.

Figure 2 displays the diagonal element of the density matrix ρ_{ii} , which represents the atomic positional distribution satisfying the sum rule $\sum_{i=1}^{N_{\text{site}}} \rho_{ii} = N_{\text{atom}}$. For $\bar{f} = 0.5$ and $\bar{f} = 0.375$ corresponding to the unstable regime, the numerical solution automatically converges to a two-phase coexistence of high-density liquid domain and low-density gas domain, with an interface in between. The average densities in the liquid and gas domains agree with f_{liq} and f_{gas} , respectively, as listed above. For $\bar{f} = 0.275$, corresponding to the metastable region, we obtain both homogeneous and inhomogeneous solutions depending on the initial conditions. The nearly homogeneous initial condition described above leads to the homogeneous solution; the inhomogeneous solution, representing a liquid droplet immersed in the background gas, is obtained when the simulation is started with a domain structure calculated separately at lower temperatures. The Helmholtz free energy $F \equiv E - TS$ per atom of the inhomogeneous solution turns out lower than that of the homogeneous one by

$0.003|v|$, corroborating that the homogeneous phase is indeed metastable.

The computed values of the chemical potential μ are presented in Fig. 3. In the pure gas phase $\bar{f} < f_{\text{gas}}$ and liquid phase $\bar{f} > f_{\text{liq}}$, we have obtained homogeneous solutions in agreement with (11). In the unstable region $f_{<} < \bar{f} < f_{>}$, we have inhomogeneous solutions with constant $\mu (= -0.15k_{\text{B}}T)$ equal to the value at two-phase coexistence. In the metastable regime $f_{\text{gas}} < \bar{f} < f_{<}$ or $f_{>} < \bar{f} < f_{\text{liq}}$, the global free-energy minimum should correspond to inhomogeneous solutions, but only homogeneous solutions could be obtained in the vicinity of the binodal $\bar{f} \approx f_{\text{gas}}, f_{\text{liq}}$; this implies that the droplet becomes too small due to the limited system size. We also note that a slight deviation of μ from the coexistence value can be observed for inhomogeneous solutions in the metastable regime, which may also be due to the smallness of the system size. Analogous plot of $-\Omega$, which is proportional to the pressure, is indicated in Fig. 4. In bulk two-phase coexistence at $k_{\text{B}}T/|v|=0.2$, the grand potential in both phases should be equal to $\Omega/N_{\text{site}}k_{\text{B}}T = -0.104$, whereas the computed values of Ω in both metastable and unstable regions are slightly higher (i.e., $-\Omega$ is lower) than this value; the difference accounts for the interfacial energy.

Figure 5 illustrates the density of states $D(\varepsilon) \equiv \sum_b \delta(\varepsilon - \varepsilon_b)$, where the delta function has been replaced by a Lorentzian of width $4 \times 10^{-3}|v|$. We find that the inhomogeneous domain structures shown in Fig. 2 are manifested by double-peak structures in the energy spectra. The lower peak can be identified as the liquid domain, $\varepsilon_{\text{liq}}/|v| = -0.655$, whereas the upper peak corresponds to the gas domain, $\varepsilon_{\text{gas}}/|v| = 0.055$; these energy levels coincide with the homogeneous solution $\varepsilon = \alpha - |v|\bar{f}$ applied to each domain ($\bar{f} = f_{\text{liq}}, f_{\text{gas}}$). A series of small peaks confined between the two main peaks may originate from the interfacial region. As \bar{f} approaches the low-density gas phase, the liquid peak is diminished and the gas peak is enhanced, which means that the fraction of gas domain increases. Eventually, only a single peak remains when the system reaches a homogeneous one-phase state. It is thus suggested that the phase stability may be probed through observing the shape of the single-particle energy spectrum.

The energy spectrum at a lower temperature, $k_{\text{B}}T/|v|=0.02$, is shown in Fig. 6 for $\bar{f} = 0.5$. Again, the double-peak structure can be observed. The Fermi distribution is now

close to a step function and hence the population of the gas domain is negligibly small. This feature is consistent with the fact that the coexisting densities approach $f_{\text{liq}} \rightarrow 1$ and $f_{\text{gas}} \rightarrow 0$ at low temperatures; the gas domain is almost vacant.

Finally, to elucidate the quantum tunneling effects, the energy spectra for $\beta/\alpha = -0.1$ and -0.01 are compared at $k_{\text{B}}T/|v| = 0.02$ in Fig. 6. It can be found that the principal effect of quantum tunnelling is to broaden the energy spectrum, similar to the electronic band-structure effects in molecules or solids. The quantum effect also acts to increase the pressure and to reduce the critical temperature, but the influence turns out small for ordinary atomic lattice gas satisfying $|v| \gg |\alpha| \gg |\beta|$: Even for a relatively strong tunnelling $\beta/\alpha = -0.5$, our numerical equations of state predict that $k_{\text{B}}T_c/|v| = 0.240$, which is still comparable to the classical mean-field value, 0.25.

3. Discussion and concluding remarks

In addition to the thermal HF theory, Mermin also developed the thermal density-functional theory (DFT) [17]. In the DFT of classical inhomogeneous fluids [18,19], a simple damping algorithm analogous to that introduced in Sec. 2.2 has been proposed to compute atomic density profiles under external fields [18]. It has been pointed out that, if the damping were neglected, a local density could take an unphysical (e.g., negative) value, leading to a breakdown of the iterative routine [18]. In the cluster-variational method [7,20,22], a classical lattice model taking account of multibody correlations beyond HF approximation, the natural iteration method has been adopted as a stable algorithm [20]; inhomogeneous phase separation in alloys has thereby been computed [20].

While the relevant parameter in DFT is a scalar density $\rho(\mathbf{r})$, the HF theory is described by the density matrix $\boldsymbol{\rho}$. In this paper, a self-consistent equation for $\boldsymbol{\rho}$ in quantum lattice gas has been presented in the form equivalent to the Roothaan equation and, by means of the simple damping algorithm, convergent iterative solutions have been obtained in the phase-separation regime; extension of the original analysis by Mermin [2] to inhomogeneous cases has thereby been achieved. Validity of the numerical results have been

confirmed in nearly classical case through comparison with the known analytic equations of state. It has been shown that the chemical potential and grand potential take on nearly constant values throughout the phase-separation region, in agreement with the general features of first-order phase transitions. Emergence of a double-peak structure in the single-particle energy spectrum would be considered as an indicator of inhomogeneities associated with phase separation. Generally, the matrix nature of ρ would play an essential role in quantum systems. In this work, broadening of the density of states due to quantum tunneling effect has been additionally demonstrated.

The present algorithm would facilitate direct numerical access to phase-transition regions of various quantum/classical systems without causing breakdown. As a potential application of the present method, we mention the gas-liquid transition of a fluid metal, a two-component system of Fermi-degenerate electrons and nearly classical ions, whose estimated critical temperatures are so high ($T_c > 10^3$ K) that experimental phase diagrams have not been established except for several elements [21,22]. First-order metal-insulator transitions [23] and other electronic topological transitions on a lattice [24] may also be studied through extension of this work. These are issues to be investigated in the future.

References

- [1] R. G. Parr and W. Yang, *Density-Functional Theory of Atoms and Molecules* (Oxford Univ. Press, 1994), Sec. 3.6.
- [2] N. D. Mermin, *Ann. Phys.* **21**, 99 (1963).
- [3] P. Bonche and D. Vautherin, *Nucl. Phys. A* **372**, 496 (1981).
- [4] B.V. Bondarev, *Physica A* **184**, 205 (1992).
- [5] I. Vidaña and A. Polls, *Phys. Lett. B* **666**, 232 (2008).
- [6] J.S. Langer, in *Solids Far From Equilibrium*, edited by C. Godrèche (Cambridge Univ. Press, Cambridge, 1992), Chap. 3.
- [7] D.A. Lavis and G.M. Bell, *Statistical Mechanics of Lattice Systems I* (Springer, Second, Revised and Enlarged Ed., 2010), Chapters 5 and 7.
- [8] A.J. Archer and R. Evans, *J. Chem. Phys.* **121**, 4246 (2004).
- [9] P. Echenique and J.L. Alonso, *Mol. Phys.* **105**, 3057 (2007).
- [10] E. Cancès and C. Le Bris, *Int. J. Quant. Chem.* **79**, 82 (2000).
- [11] D.R. Hartree, *The Calculation of Atomic Structures* (John Wiley & Sons, NY., 1957), Chap. 5.
- [12] V.R. Saunders and J.H. Hiller, *Int. J. Quant. Chem.* **7**, 699 (1973).
- [13] P. Pulay, *J. Comp. Chem.* **3**, 556 (1982).
- [14] K.N. Kudin, G.E. Scuseria, and E. Cancès, *J. Chem. Phys.* **116**, 8255(2002).
- [15] X. Hu and W. Yang, *J. Chem. Phys.* **132**, 054109 (2010).
- [16] T. Husch, A.C. Vaucher, and M. Reiher, *Int. J. Quant. Chem.* **118**, 25799 (2018).
- [17] N.D. Mermin, *Phys. Rev.* **137**, A1441 (1965).
- [18] A.P. Hughes, U. Thiele, and A.J. Archer, *Am. J. Phys.* **82**, 1119 (2014).
- [19] J.-L. Barrat and J.-P Hansen, *Basic Concepts for Simple and Complex Liquids* (Cambridge Univ. Press, Cambridge, 2003), Chap. 7.
- [20] T. Mohri, *JOM* **65**, 1510 (2013).
- [21] F. Hensel and W.W. Warren, Jr., *Fluid Metals* (Princeton Univ. Press, Princeton, 1999).
- [22] H. Kitamura, *Comp. and Math. Methods* **1**, 1011 (2019).
- [23] Y. Shi and L.-Q. Chen, *Phys. Rev. B* **102**, 195101 (2020).

[24] J. Wen, A. Rüegg, C.-C.J. Wang, and G.A. Fiete, *Phys. Rev. B* **82**, 075125 (2010).

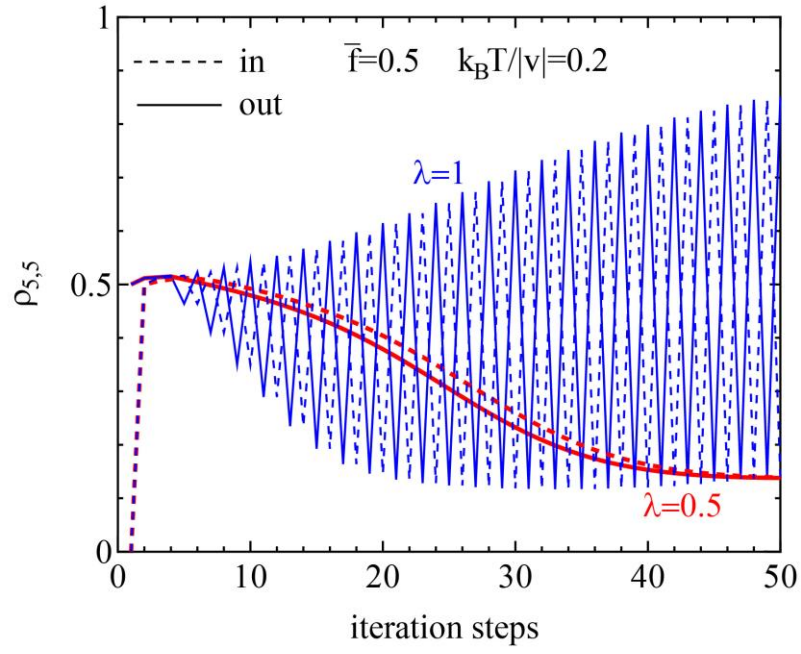


Figure 1. Evolutions of $\tilde{\rho}_i^{\text{in}}$ (dotted lines) and ρ_{ii}^{out} (solid lines) for $i=5$ during iterations. The cases $\lambda=1$ and 0.5 are compared.

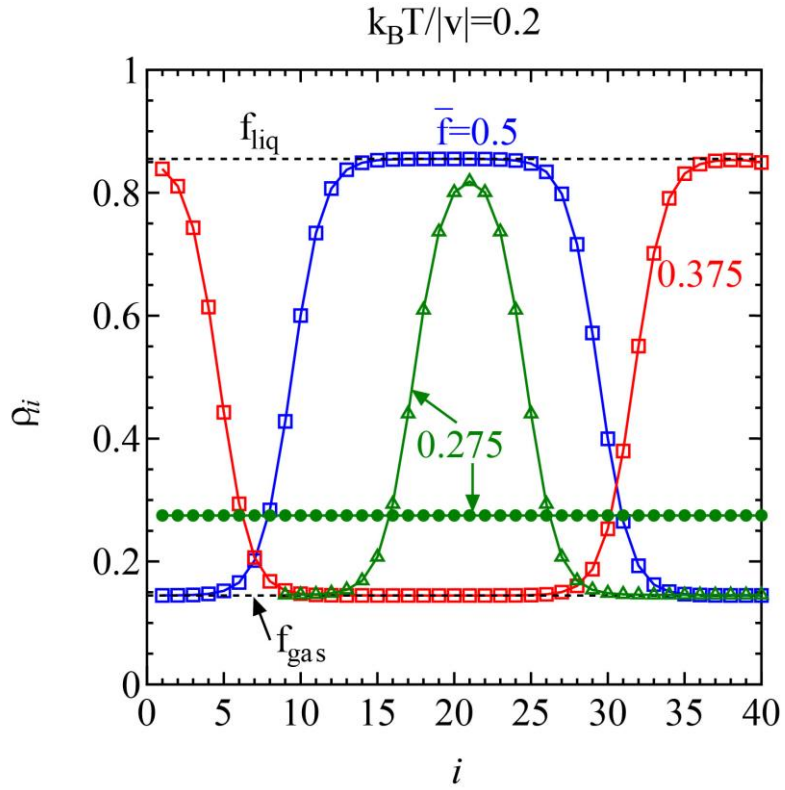


Figure 2. Atomic site distributions for various average densities. Filled circles represent homogeneous solutions; squares and triangles indicate inhomogeneous solutions in unstable and metastable regions, respectively. The connecting lines are for guides to the eyes. The homogeneous densities of the coexisting liquid and gas phases are indicated by horizontal dotted lines.

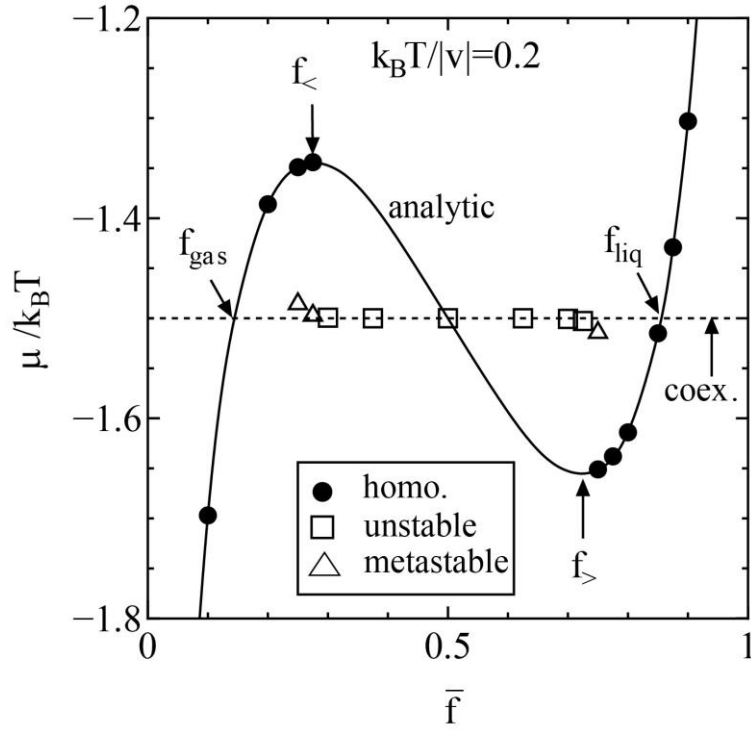


Figure 3. Chemical potential as a function of average density. Filled circles depict homogeneous solutions; squares and triangles indicate inhomogeneous solutions in unstable and metastable regions, respectively. Solid curve represents Eq. (11). Dotted line stands for the coexistence condition.

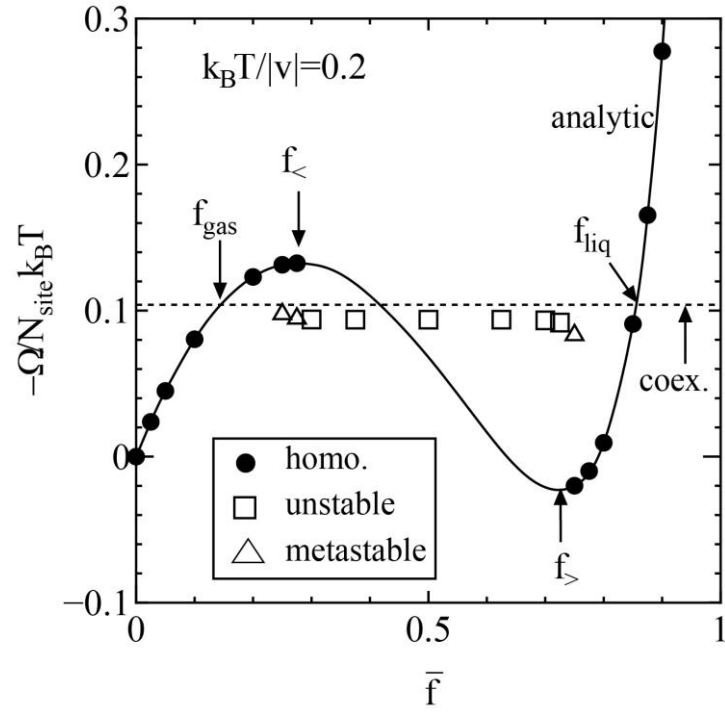


Figure 4. Negative of the grand potential as a function of average density. Solid curve depicts Eq. (10). The definitions of symbols are otherwise the same as Fig. 3.

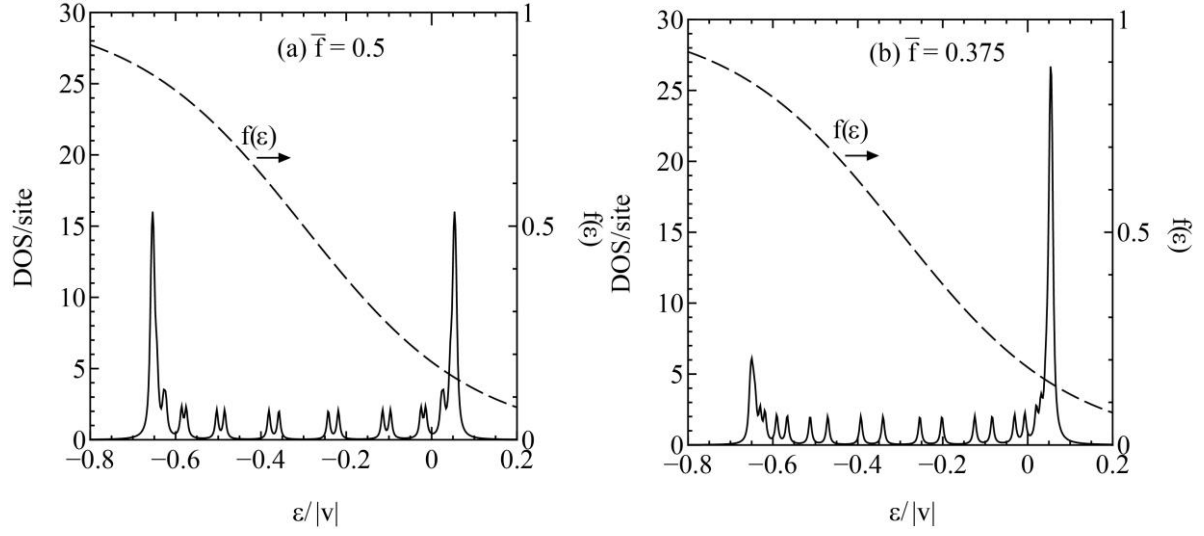


Figure 5. Density of states per site for (a) $\bar{f} = 0.5$ and (b) $\bar{f} = 0.375$; the temperature is $k_{\text{B}}T/|v| = 0.2$ in both cases. Dashed curves depict the Fermi distribution, Eq. (5).

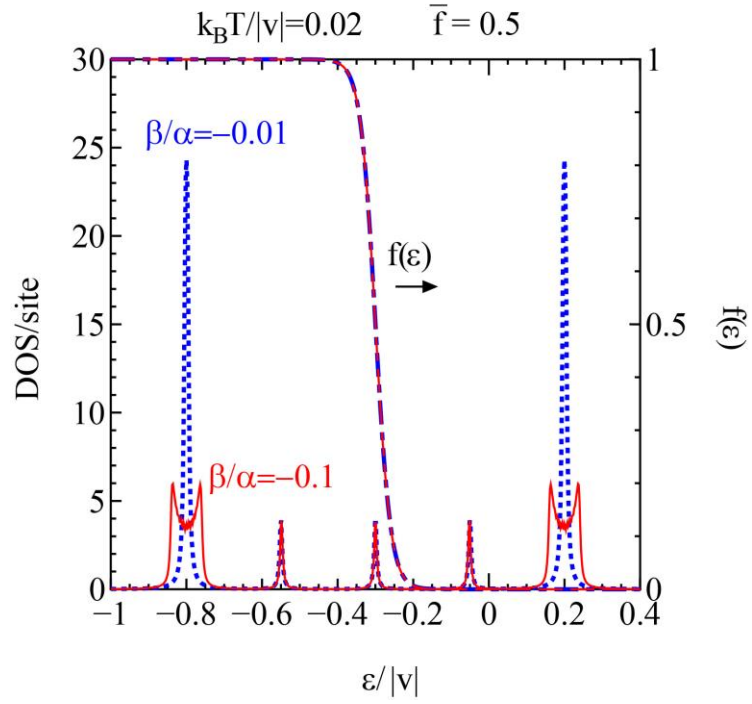


Figure 6. Density of states per site for $k_B T/|v|=0.02$ and $\bar{f}=0.5$. Solid and dotted curves indicate the case $\beta/\alpha = -0.1$ and -0.01 , respectively; dashed and dot-dashed curves are the Fermi distributions for the respective cases.